Available online at www.sciencedirect.com

SCIENCE DIRECT®

Polymer 46 (2005) 6897–6909

polymer

www.elsevier.com/locate/polymer

Photocrosslinking of poly(ethylene terephthalate) copolymers containing photoreactive comonomers

Junzuo Wang[a], Bishwa R. Nayak[a], David Creed[b], Charles E. Hoyle[a,b], Lon J. Mathias[a,*]

[a]*Department of Polymer Science, The University of Southern Mississippi, Southern Station Box 10076, 2609 West 4th Street, Hattiesburg, MS 39406, USA*
[b]*Department of Chemistry and Biochemistry, The University of Southern Mississippi, Hattiesburg, MS 39406, USA*

Received 21 March 2005; received in revised form 15 June 2005; accepted 16 June 2005
Available online 18 July 2005

Abstract

Poly(ethylene terephthalate) (PET) copolymers containing 4,4′-, 3,5-, and 2,4-benzophenone dicarboxylate chromophores have been synthesized by transesterification of PET with benzophenone 4,4′-dicarboxylic acid (4,4′-BDA), dimethyl benzophenone 4,4′-dicarboxylate (4,4′-BDE), dimethyl benzophenone 3,5-dicarboxylate (3,5-BDE) and dimethyl benzophenone 2,4-dicarboxylate (2,4-BDE). The benzophenone segments in the backbone induce photocrosslinking upon UV irradiation in the solid state most probably by a hydrogen atom abstraction mechanism. The crosslinking rate depends upon the concentration and the structure of chromophores as evidenced by gel content measurements. The photocrosslinking efficiency of 4,4′-benzophenone dicarboxylate containing polymers is higher than for 2,4- or 3,5-benzophenone dicarboxylate containing polymers. Photocrosslinked PET copolymers show increased glass transition temperatures and broadening of melting transitions.

Keywords: Poly(ethylene terephthalate) copolymers; Benzophenone chromophores; Photocrosslinking

1. Introduction

Thermoplastic polymers have the advantages of high tenacity, reprocessability, and high impact strength while thermoset polymers show low shrinkage, high heat deflection temperature and high modulus. Controlled crosslinking of linear polymers offers advantages for both thermoplastic and thermoset polymers. Crosslinking of polyethylene [1–4], polystyrene [5], polyimides [6,7], polyphosphazenes [8,9], liquid crystalline polymers [10, 11], PET [12–14], and poly(butylene terephthalate) [12], have been extensively reported. PET is an important engineering plastic with applications ranging from textiles to bottles and reinforced fibers. Highly oriented PET fibers in car tires maintain dimensional stability of the tire, and enhance modulus and strength, which provide better performance and greater safety. PET is a semi-crystalline polymer with a glass transition of around 78 °C. Highly oriented PET fiber has a glass transition around 110 °C. In hot climates and under high speed driving conditions, the temperature inside a car tire may exceed 110 °C. The strength and modulus of PET fibers decrease dramatically above the glass transition temperature, and high modulus fibers are needed to meet these harsh conditions. Specifically, high heat deflection temperature, low shrinkage and high modulus PET fibers are required for this and related applications.

There are several approaches to achieving those goals: PET composites can be made with inorganic fillers such as clay [15] or POSS (polyhedral silsesquioxane) [16]. Multifunctional monomers may be incorporated into the PET backbone [17]. Incorporation into PET of photoreactive comonomers which will photocrosslink after processing has also been reported [12–14]. The first approach is in principle easiest since clay or POSS can be fed directly into the polymerization reaction. However, inorganic fillers and PET have compatibility problems and few organically-modified fillers can withstand the synthesis or processing conditions of PET polymerization (high temperature and catalysts). With the second approach, different degrees of crosslinking can be obtained by varying the ratio of multifunctional monomers to difunctional monomers. However,

---

[*] Corresponding author. Tel.: +1 601 266 4871; fax: +1 601 266 5635.
E-mail address: lon.mathias@usm.edu (L.J. Mathias).

0032-3861/$ - see front matter © 2005 Elsevier Ltd. All rights reserved.
doi:10.1016/j.polymer.2005.06.043

branched or lightly crosslinked fibers and films are hard to process or cannot be formed at all. The last approach requires careful selection of photoreactive comonomers. These must be able to withstand the high temperatures required for PET polymerization and should be incorporated in low enough concentrations so that the desirable physical properties of PET are not greatly perturbed.

Photocrosslinking of PET copolymers by cycloaddition of incorporated cinnamic acid analogs has been reported [12]. For example, 1,4-phenylene-bis-(acrylic acid) is a thermally stable monomer that has been incorporated into PET and that can bring about crosslinking by an ‘allowed’ [2+2] photocycloaddition. However, effective crosslinking requires two alkene-like double bonds on different polymer chains to be close to one another and at a rather specific orientation (‘topochemical control’), and at low overall concentration, the photocrosslinking efficiency of polymers may be low.

Linear polymers can be photocrosslinked by benzophenone [1–4]. The crosslinking mechanism most probably involves hydrogen atom abstraction by the benzophenone triplet state. This is the most widely encountered photochemical reaction of benzophenone [18]. Following UV excitation to the excited singlet state, intersystem crossing occurs with unit efficiency providing a much longer lived triplet state which is a potent hydrogen atom abstractor. Benzophenone groups can be incorporated into PET as main chain or as pendent moieties, or bound to the ends of PET chains. The copolymers can be processed into films or fibers using established methods. Although the crosslinking of PET copolymers containing 4,4′-benzophenone dicarboxylic acid methyl ester and *N*,*N*′-bis(hydroxyethyl) benzophone teracarboxylic acid diimide have been reported [19–21], substituent effects of benzophenone chromophores as main chain and pendent groups on photocrosslinking efficiencies have not been reported.

In this paper we report the incorporation of various concentrations of 4,4′-, 3,5-, and 2,4-benzophenone dicarboxylate chromophores into PET by transesterification of PET with benzophenone 4,4′-dicarboxylic acid (4,4′-BDA), dimethyl benzophenone 4,4′-dicarboxylate (4,4′-BDE), dimethyl benzophenone 3,5-dicarboxylate (3,5-BDE) and dimethyl benzophenone 2,4-dicarboxylate (2,4-BDE). The 4,4′-benzophenone dicarboxylate is an example of a chromophore wholly incorporated into the main chain of the polymer. The 3,5- and 2,4-benzophenone dicarboxylate chromophores are examples of chromophores that are at least partly pendent to the PET main chain. The UV absorption spectra of these copolymers before and after photoirradiation were studied. UV irradiations of pressed films were conducted above 320 nm so as to minimize PET degradation by direct excitation of the terephthalate chromophore [22]. Gel content measurements were used to study the relative rates of photocrosslinking of the different polymers. In general the 4,4′-benzophenone dicarboxylate chromophore led to faster crosslinking than the 3,5- and 2,4-benzophenone dicarboxylate chromophores. Increased concentrations of chromophores led to faster crosslinking. Thermal analysis methods were used to compare the thermal and mechanical properties of unirradiated and photoirradiated samples. The irradiated, crosslinked polymers showed higher glass transition temperatures and high-temperature moduli than the unirradiated uncrosslinked polymers.

2. Experimental

2.1. Materials

All starting materials and solvents were purchased from Aldrich and Acros Chemical Co. 4,4′-BDA and 3,5-dimethyl benzoic acid were obtained from TCI Co.

2.2. Synthesis

2.2.1. Dimethyl 4,4′-benzophenonedicarboxylate (4,4′-BDE)

Benzophenone 4,4′-dicarboxylic acid (4.05 g, 15 mmol) and thionyl chloride (23 ml, 315 mmol) were refluxed for 2 h and excess thionyl chloride was removed by reduced-pressure distillation. Dry toluene (20 ml) was added to dissolve the benzophenone 4,4′-dicarboxylic acid chloride. Dry methanol (2.43 ml, 60 mmol), pyridine (5 ml, 62 mmol) and toluene (10 ml) were added dropwise. After addition, the system was refluxed overnight. The solution mixture was cooled to room temperature and a white powder was obtained. The product was washed with $NaHCO_3$ solution (5 wt% in H_2O), water and dried in a vacuum oven until a constant weight was obtained. The product was further recrystallized from toluene. Yield: 64%, mp 240–244 °C (Ref. [23] mp 224–225 °C). ^1H NMR (TFA, δ): 8.1–8.2 (4H, Ar-H3,3′,5,5′); 7.8–7.9 (4H, Ar-H2,2′,6,6′); 4.9 (6H, CH_3). ^{13}C NMR (TFA, δ): 194.2 (ketone); 162.8 (carbonyl); 133.5, 126.9, 123.7, 123.2 (aromatic carbons); 46.3 (CH_3). FTIR (KBr, cm^{-1}): 2956 (C–H), 1730 (ester carbonyl), 1649 (ketone), 1279 and 1105 (C–O). Anal. Calcd for $C_{17}H_{14}O_5$: C, 68.45; H, 4.73. Found: C: 67.90; H, 4.54. The overall synthesis is shown in Scheme 1.

2.2.2. Benzophenone 2,4-dicarboxylic acid (2,4-BDA)

Potassium permanganate (50.6 g, 0.32 mol in 200 ml H_2O) was heated to 90 °C. 2,4-Dimethyl benzophenone (25.14 g, 0.12 mol) and pyridine (300 ml) were added dropwise. During addition, potassium permanganate (101.2 g, 0.64 mol) in H_2O (400 ml) was added over 3 h. After addition of potassium permanganate was complete, the reaction was allowed to continue for 6 h. The system was allowed to cool down and the solid product was vacuum filtered. The filtrate was washed several times with hot water. The solution was neutralized to pH 7 to give crude benzophenone 2,4-dicarboxylic acid. The precipitate was recrystallized from

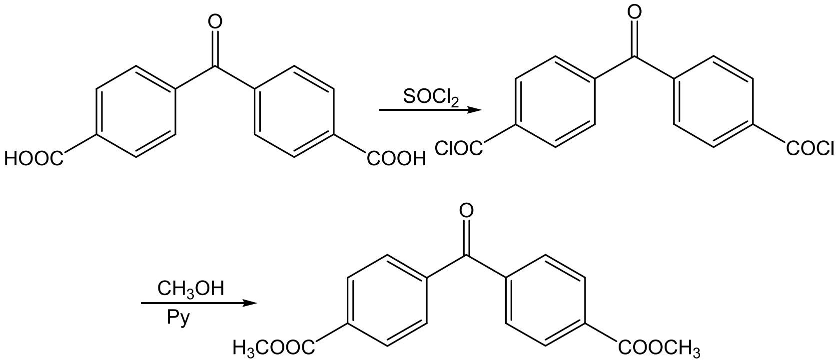

Scheme 1. Synthesis of dimethyl 4,4′-benzophenonedicarboxylate.

acetic acid. Yield: 40%. ^{1}H NMR (DMSO-d_6, δ): 13.5 (acid); 8.5–7.5 (aromatic protons). ^{13}C NMR (DMSO-d_6, δ): 196.5 (ketone); 166.7 (carbonyl); 128.6–145.9 (aromatic carbons). FTIR (KBr, cm^{-1}): 2991–2540 (C–H), 1695 (ester carbonyl and ketone), 1279 and 1244 (C–O).

2.2.3. *Dimethyl 2,4-benzophenonedicarboxylate (2,4-BDE)*

Benzophenone 2,4-dicarboxylic acid (20.51 g, 0.076 mol), dry methanol (300 ml) and H_2SO_4 (96%, 16 ml) were refluxed for about 20 h (Scheme 2). The methanol solution was cooled and dimethyl 2,4-benzophenone dicarboxylate precipitated. The product was filtered and washed with $NaHCO_3$ solution (5 wt% in water) and then water to give dimethyl 2,4-benzophenonedicarboxylate. The product was obtained from methanol as white crystals 17.5 g (77%), mp 119–122 °C. ^{1}H NMR (DMSO-d_6, δ): 8.5–7.50 (aromatic protons); 3.9–3.6 (CH_3). ^{13}C NMR (DMSO-d_6, δ): 196.0 (ketone); 165.6 (carbonyl); 145.8–129.1 (aromatic carbons); 53.4–53.2 (CH_3). FTIR (KBr, cm^{-1}) 2956 (C–H), 1730 (ester carbonyl), 1672 (ketone), 1244 and 1117 (C–O).

2.2.4. *3,5-Dimethylbenzophenone [24]*

3,5-Dimethyl benzoic acid (15.02 g, 0.1 mol) and thionyl chloride (125 ml) were refluxed overnight. The excess thionyl chloride was removed by reduced-pressure distillation and a brown solid (3,5-dimethyl benzoyl chloride) precipitated upon cooling. The precipitate was dissolved in dry benzene (40 ml) and the solution added dropwise to anhydrous aluminum chloride (16.7 g, 0.125 mol) in dry benzene (60 ml) at ambient temperature. The mixture was heated gently during acid chloride addition then refluxed overnight. The mixture was cooled to room temperature and concentrated HCl and water (1:1 by volume) were added slowly to the ice cooled reaction flask. The benzene layer was separated from water layer and water layer was washed with benzene twice. The combined benzene layers were dried ($MgSO_4$, 6 g) overnight. The benzene was removed from the solution mixture by reduced pressure distillation. A brown solid product was obtained which was recrystallized from hexane (50 ml) containing activated carbon (0.2 g) to give the pure 3,5-dimethylbenzophenone as light yellow crystals, 16.3 g (78%). mp 65–67 °C (Ref. [24] mp 70–71 °C). ^{1}H NMR ($CDCl_3$, δ): 7.8–7.2 ppm (aromatic protons); 2.4 ppm (single peak, CH_3). ^{13}C NMR ($CDCl_3$, δ): 197.4 (ketone); 138.2–128.0 (aromatic carbons) and 21.5 (CH_3). FTIR (KBr, cm^{-1}): 2866, 2916 and 3059 (C–H), 1659 (ketone), 1232 and 1136 (C–O).

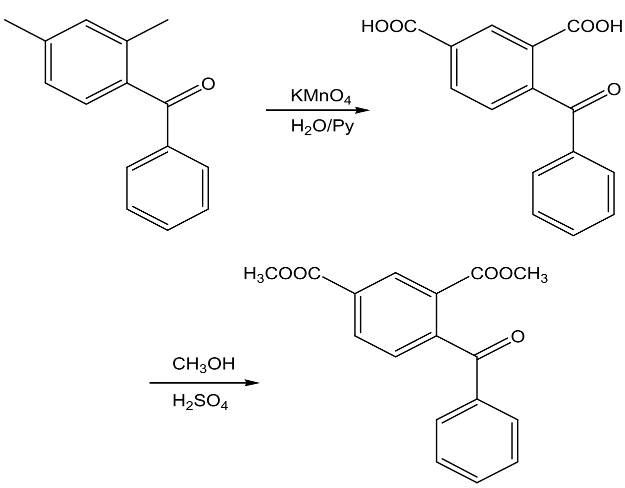

Scheme 2. Synthesis of dimethyl 2,4-benzophenonedicarboxylate.

2.2.5. *Benzophenone 3,5-dicarboxylic acid (3,5-BDA)*

The procedure was similar to that used for the synthesis of benzophenone 2,4-dicarboxylic acid. Potassium permanganate (13.13 g, 0.083 mol) in water (60 ml) was heated to 90 °C. 3,5-Dimethyl benzophenone (6.3 g, 0.03 mol) and pyridine (80 ml) were added dropwise. Additional potassium permanganate and water were added several times before completion of reaction. The crude product was recrystallized from acetic acid to give purified benzophenone 3,5-dicarboxylic acid. The yield of white crystals was 4.7 g (58%). ^{1}H NMR (DMSO-d_6, δ): 13.4 (carboxylic acid); 8.7–7.6 ppm (aromatic protons). ^{13}C NMR (DMSO-d_6, δ): 195.0 (ketone); 166.5 (carbonyl); 138.4–129.4 ppm (aromatic carbons).

2.2.6. *Dimethyl 3,5-benzophenonedicarboxylate (3,5-BDE)*

The procedure was similar to that used for synthesis of dimethyl 2,4-benzophenonedicarboxylate. 3,5-Benzophenone dicarboxylic acid (0.98 g, 0.004 mol), dry methanol (20 ml) and H_2SO_4 (96%, 0.8 ml) were refluxed for about 20 h. The solution mixture was cooled and dimethyl 3,5-benzophenone dicarboxylate precipitated out. The product was filtered and recrystallized from methanol. Yield of white crystals was 0.7 g (65%), mp 110–116 °C. ^{1}H NMR (DMSO-d_6, δ): 8.6–7.6 ppm (aromatic protons); 3.9 (OCH_3). ^{13}C NMR (DMSO-d_6, δ): 195.0 (ketone); 165.3 (carbonyl); 138.7–129.5 ppm (aromatic carbons); 54.0 (CH_3). FTIR (KBr, cm^{-1}): 2956 (C–H), 1724 (ester carbonyl), 1660 (ketone), 1255 and 1157 (C–O). Anal. Calcd for $C_{17}H_{14}O_5$: C, 68.45; H, 4.73. Found: C: 68.26; H, 4.56 (Scheme 3).

2.2.7. PET/BDA copolymers

The PET/BDA copolymers were prepared by the following transesterification reaction [13]. Dimethyl terephthalate (777 g, 4.0 mol), ethylene glycol (521 g, 8.40 mol), $Mn(CH_3CO_2)_2.4H_2O$ (0.277 g, 1.29 mmol), and Sb_2O_3 (0.358 g, 1.23 mmol) were heated for 2 h at 180–210 °C, during which methanol was removed by distillation. Polyphosphoric acid (0.168 g) was added, and the pressure was slowly reduced to 1 mmHg over 40 min. The reaction mixture was heated to 280–290 °C for an additional 2 h. After ethylene glycol was completely removed, a specific weight percentage of 4,4′-BDA was added into the reaction mixture (Table 1). The reaction was continued for 0.5 h at 280–290 °C under reduced pressure. The polymer was extruded from the reaction vessel under a positive pressure of nitrogen. The copolymer was cut into pellets and heated to 220 °C for 24 h under reduced pressure to induce solid state polymerization (SSP). ^{1}H NMR (TFA) δ 8.0 (4H, ArHs in terephthalate and 4H, 3,3′,5,5′ ArHs in benzophenone 4,4′-dicarboxylate units); 7.8 and 7.7 (4H, 2,2′,6,6′ ArHs in benzophenone 4,4′-dicarboxylate units) and 4.7 ppm (4H, CH_2CH_2 units). ^{13}C NMR (TFA) δ 165.0 (carbonyl), 129.8 and 125.9 (aromatic carbons) and 60.0 ppm (aliphatic carbons). FTIR (cm^{-1}): 2968 (C–H), 1730 (ester carbonyl), 1695 (ketone), 1267 and 1105.0 (C–O). As an example of the notation used in this work a PET copolymer denoted as PET/4,4′BDA-18, SSP has 18% incorporation of 4,4′-BDA by weight with solid state polymerization. All polymers synthesized are listed in Table 1.

2.2.8. PET/BDE copolymers

The procedure for synthesizing PET/BDE copolymers (PET/2,4BDE-4, PET/3,5BDE-4, PET/4,4′BDE-4) was similar to that used for PET/4,4′BDA-4 copolymer except that the BDE comonomers were added to dimethyl terephthalate and ethylene glycol at the very beginning of polymerization. Solution NMR spectra of PET/4,4′BDA-4 and PET/4,4′BDE-4 are almost identical as are the FTIR spectra. All polymers synthesized are listed in Table 1 (Scheme 4).

2.3. Polymer film preparation

Amorphous films of PET copolymers were prepared by quenching PET copolymer melt pressed films (280 °C) between two cold metal plates or into liquid nitrogen.

2.4. Irradiations of polymer films

Amorphous films of PET and PET copolymers were irradiated either with a high-intensity UV lamp or low-intensity UV lamp. Glass filters were used to avoid excitation of the terephthalate chromophore at the indicated temperatures and times, and then quenched to room temperature. The high-intensity UV source was a Power Cure™ 3 UV medium pressure mercury lamp with D bulb manufactured by Fusion UV Systems, Inc. MD, USA that

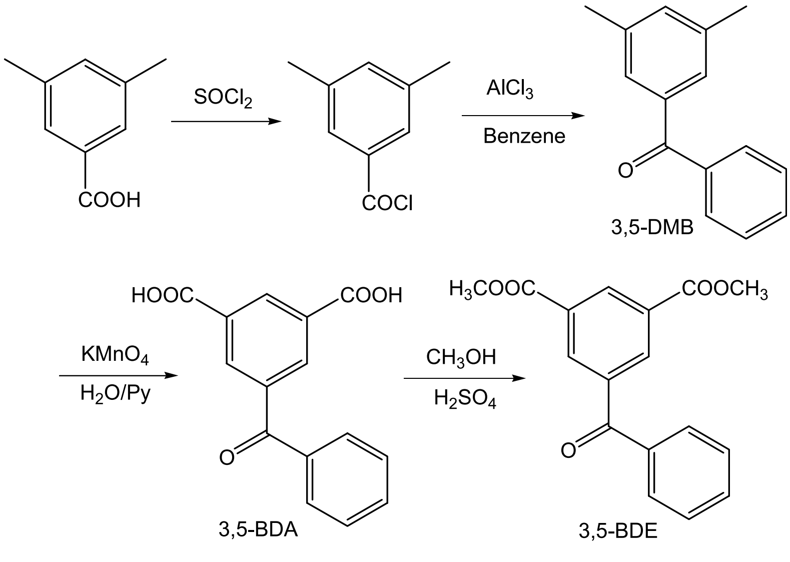

Scheme 3. Synthesis of dimethyl 3,5-benzophenonedicarboxylate.

Table 1
Characterization of PET copolymers

Copolymers	η_{iv}[a] (dl/g)	BDA (or BDE) feed		Composition[b] of BDA (or BDE)		T_g[c]/°C	T_c[c]/°C	T_m[c]/°C	T_d[d] (2.5%)/°C	T_d (5%)/°C
		mol%	wt%	mol%	wt%					
PET, SSP[e]	0.80	0	0	0	0	76.0	122.2	253.0	388.9	398.8
PET/4,4′BDA-4, SSP	0.84	3	4.0	2.3	3.3	76.7	129.8	246.7	384.4	393.5
PET/4,4′BDA-6.5, SSP	0.85	5	6.5	4.5	6.2	77.2	134.4	242.2	386.4	396.5
PET/4,4′BDA-6.5, non-SSP[f]	0.71	5	6.5	4.6	6.3	76.1	131.6	243.8	387.4	397.3
PET/4,4′BDA-18, non-SSP	0.61	13.8	18	13.7	18.0	80.0	142.1	223.5	384.4	395.7
PET/4,4′BDE-4, non-SSP	0.60	2.6	4	2.3	3.6	77.5	125.4	249.7	386.7	395.0
PET/3,5BDE-4, non-SSP	0.63	2.6	4	1.8	3.2	76.8	125.4	249.5	384.4	392.7
PET/2,4BDE-4, SSP	0.85	2.6	4	1.5	2.7	77.2	128.3	248.6	386.5	395.7

[a] Intrisic viscosity data were obtained at 25 °C using phenol/tetrachloroethane mixture as a solvent.
[b] Determined by ^{1}H NMR integration.
[c] Determined by DSC at 10 °C/min under N_2.
[d] Determined by TGA at 10 °C/min under N_2.
[e] SSP: Solid state polymerization.
[f] Non-SSP: Non-solid state polymerization.

generated light from 200 to 600 nm; the maximum intensity of light is between 350 and 380 nm; intensity was 70 ± 25 mW/cm^2. The low-intensity UV lamps were made by Southern N.E. Ultraviolet, Branford, CT. USA. The gel contents (wt%) were determined by stirring the irradiated samples (1 wt%) in trifluoroacetic acid (TFA) at room temperature for 24 h. The insoluble gel fractions were separated by filtration, washed several times with TFA and dried above 100 °C to constant weight under vacuum.

2.5. Instrumentation

^{1}H and ^{13}C NMR spectra were obtained using a Varian Mercury 300 spectrometer operating at 300 MHz for hydrogen and 75 MHz for carbon. Infrared spectra were recorded on an ATI-Mattson Galaxy 5020 FTIR spectrometer. Thermal analyses were performed on a TA instruments SDT 2960, TGA–DTA at 10 °C/min under nitrogen from ambient temperature to 600 °C and DSC at 10 °C/min under nitrogen from ambient temperature to 300 °C. Mechanical properties of PET copolymer films (100–200 μm thickness) were carried out under tension using a Perkin–Elmer Pyris Diamond dynamic mechanical analyzer. The heating rate was 2 °C/min and the frequency was 1 Hz. UV absorption spectra of solutions and films of PET copolymers were recorded on a Shimadzu UV-2401 PC scanning spectrophotometer. Wide-angle X-ray diffraction measurements were performed on a Siemens XPD-700P diffractometer using Cu K_α radiation in the 2Θ range of 5–35°, at a sample detector distance of 30 cm.

3. Results and discussion

3.1. Monomer synthesis

Dimethyl 4,4′-benzophenonedicarboxylate (4,4′-BDE) was synthesized from 4,4′-benzophenonedicarboxylic acid (4,4′-BDA) in two steps as shown in Scheme 1 or by direct acid catalyzed esterification by methanol of 4,4′-BDA.

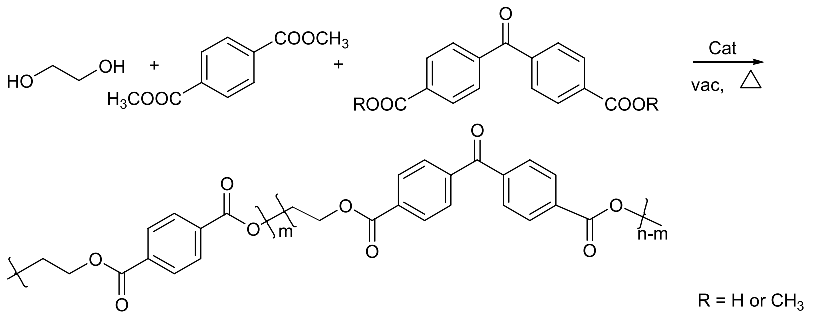

Scheme 4. Synthesis of PET/BDA (or BDE) copolymer.

The synthesis of dimethyl 2,4-benzophenone dicarboxylate (2,4-BDE) is shown in Scheme 2. Oxidation of 2,4-dimethyl benzophenone to benzophenone 2,4-dicarboxylic acid (2,4-BDA) can be conducted either in water or water/pyridine solvent mixtures. Oxidation in water led to a lower conversion of 2,4-BDA (25%), but a higher purity as determined by proton NMR analysis. Oxidation in water/pyridine gave a higher yield of 2,4-BDA (80% before recrystallization, 40% after recrystallization from acetic acid), but a lower purity. High purity 2,4-BDA (obtained by oxidation in water/pyridine) was hard to obtain by recrystallization. However, pure 2,4-BDE can be obtained by the recrystallization of esterified, impure 2,4-BDA. The ^{1}H NMR spectrum of purified dimethyl 2,4-benzophenone-dicarboxylate (2,4-BDE) indicated less than 0.5% of impurities, probably mono-ester isomers. There are two kinds of chemical shifts for methyl groups of 2,4-BDE (3.6 and 3.9 ppm in the ^{1}H NMR spectrum). Steric effects of the *ortho* linked benzoyl group might deshield one methyl ester and lead to the different chemical shifts.

Scheme 3 shows the synthesis of dimethyl 3,5-benzophenonedicarboxylate (3,5-BDE). 3,5-Dimethylbenzophenone was synthesized by Friedel-Crafts acylation of benzene by 3,5-dimethylbenzoyl chloride catalyzed with $AlCl_3$. Instead of using CH_2Cl_2 solvent as reported in the literature synthesis [24], excess benzene was used which acts both as a reactant and a solvent. Oxidation of 3,5-dimethylbenzophenone and esterification of the diacid with methanol were carried out in the same way as for the preparation of the 2,4-isomer.

3.2. Polymer characterization

Molecular weights of PET copolymers were determined by intrinsic viscosity (listed in Table 1) and calculated by the Mark–Houwink equation [25]:

$$\eta_{iv} = 7.61\times10^{-1}\ \mathrm{M}^{0.67}$$

PET and PET copolymers have molecular weights from 21,100 to 35,400.

The proton NMR spectra of the copolymers were very similar to that of PET except that we clearly observe the additional aromatic peaks due to the benzophenone chromophores. These spectra indicate incorporation of most of the benzophenone derivatives originally in the feed into the copolymers. The actual concentrations of incorporated benzophenone chromophores in the copolymers were determined by proton NMR. For example, the proton NMR spectrum of comonomer 4,4′-BDE showed two aromatic proton doublets which were widely separated [8.2–8.1 (4H, Ar-H3,3′,5,5′); 7.9 (4H, Ar-H2,2′,6,6′)]. The proton NMR spectrum for PET/4,4′BDA-4 copolymer showed three kinds of aromatic protons. One is from the terephthalate units and the other two from 4,4′-BDE segments. The resonance peak of the aromatic proton *ortho* to the carbonyl group was well separated from the other two peaks. Based on the ratios of the areas of these different peaks, the concentrations of benzophenone chromophores were determined (Table 1). The actual fractions of benzophenone chromophores determined by this proton NMR analysis were similar to those fed into the transesterification reactions. The successful incorporation of the benzophenone chromophores into PET is also shown by the new absorption above 320 nm in the UV spectra of the copolymers (vide infra).

DSC results for PET/4,4′BDA copolymers (Table 1) show increases in glass transition temperatures and decreases in melting points with increasing 4,4′-BDA concentration. The 4,4′-BDA unit is more rigid than the terephthalate unit and the incorporation of 4,4′-BDA into the PET backbone inhibits mobility of the polymer chains and, therefore, increases the glass transition temperature. 4,4′-BDA incorporated into the PET backbone at a low concentration reduces the regularity of the backbone which decreases its melting point and increases the crystallization temperature (T_c). The incorporation of 4 wt% comonomer led to a 1–2 °C increase in T_g, a 3–6 °C decrease in T_m, and no change in T_d (decomposition temperature). Thus, this level of BDA (or BDE) incorporated does not significantly impact the thermal properties of PET.

3.3. UV–vis absorption spectra of PET copolymers and monomers

It is well known that direct UV irradiation of PET results in effects such as chain cleavage, yellowing, and loss of desirable mechanical properties [22,26]. We chose the benzophenone chromophore, in part, because it absorbs at a longer wavelength than the terephthalate chromophore and most of the direct excitation of the latter in the copolymers could be avoided with filtered UV light. Fig. 1 shows the UV absorption spectra of two PET copolymer films and of pure PET. Both copolymers have a characteristic benzophenone type absorption band at much longer wavelengths than the absorption of pure PET. We, therefore, used a window glass filter to cut off exciting light below 320 nm and to prevent most of the direct excitation of the terephthalate chromophore during the photocrosslinking experiments.

It is noteworthy that the UV absorption of PET/2,4BDE-4 is much weaker than that of PET/4,4′BDA-4. The UV absorption spectra of the benzophenone diester monomers run at the same concentrations in trifluoroacetic acid solution (Fig. 2) confirmed that the UV absorption of the 2,4-BDE chromophore is shifted to the blue and has a lower molar absorptivity compared to that of the 4,4′-BDE chromophore. There are presumably two reasons for the reduced conjugation of the 2,4-BDE chromophore, which leads to these effects. The *para–para* substitution pattern of the 4,4′-BDE chromophore leads to stronger conjugation of the ketone group with the ester groups; this is reduced for the 2,4-BDE and 3,5-BDE chromophores. Furthermore the

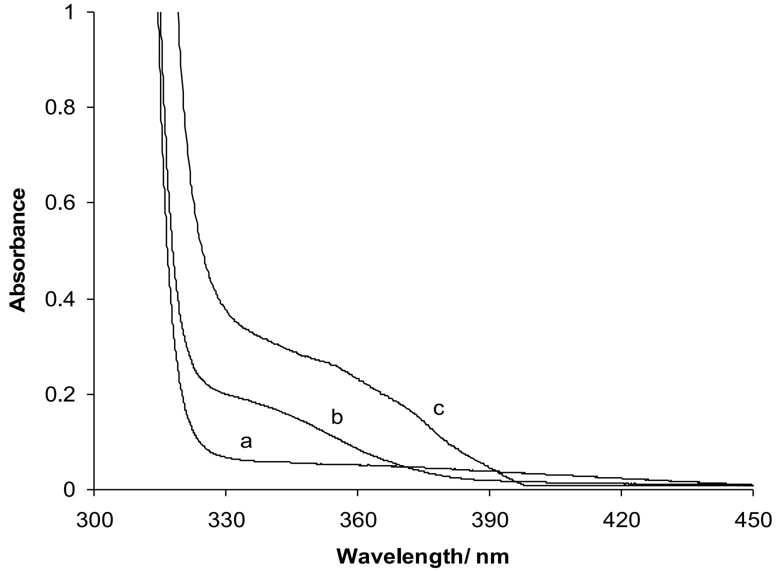

Fig. 1. UV spectra of (a) PET, (b) PET/2,4BDE-4, (c) PET/4,4BDA-4; film thicknesses: 50–80 μm.

greater twisting of the benzophenone groups of 2,4-BDE would also cause a decrease of conjugation.

3.4. Photocrosslinking of PET copolymers

PET copolymer films were irradiated with low intensity (LI) and high intensity (HI) UV lamps using window glass filters that cut out most of the light below 320 nm in order to avoid direct excitation of terephthalate units in the PET backbone. Figs. 3 and 4 shows the percentage gel content as a function of irradiation time for the irradiated amorphous PET/4,4′BDA (SSP) films with LI and HI UV lamps. Crosslinking kinetics of PET/4,4′BDA-4 (SSP) and PET/4,4′BDA-6.5 (SSP) show a similar pattern; i.e. a fast initial increase in gel content within 1 h for PET/4,4′BDA-4 (SSP) with LI UV lamps, a slow increase between 1 and 4 h, and no further gel formation after 4 h of irradiation. The photocrosslinking rate depends on the concentration of benzophenone chromophores as evidenced from the higher gel content for PET/4,4′BDA-6.5 (SSP) than PET/4,4′BDA-4 at similar irradiation times with HI UV lamp. The photocrosslinking rate also depends on the chemical structure of the benzophenone chromophore. PET/4,4′BDE-4 has 70% gel content, PET/3,5BDE-4 has 30% gel content, whereas PET/2,4BDE-4 does not have any gel content with 8 h of irradiation with LI UV lamps.

Fig. 5 shows the UV absorption spectra of PET and PET/4,4′BDA-4 copolymer films before and after photoirradiation. The absorption spectra for PET are almost identical while the irradiated PET/BDA copolymers show strong

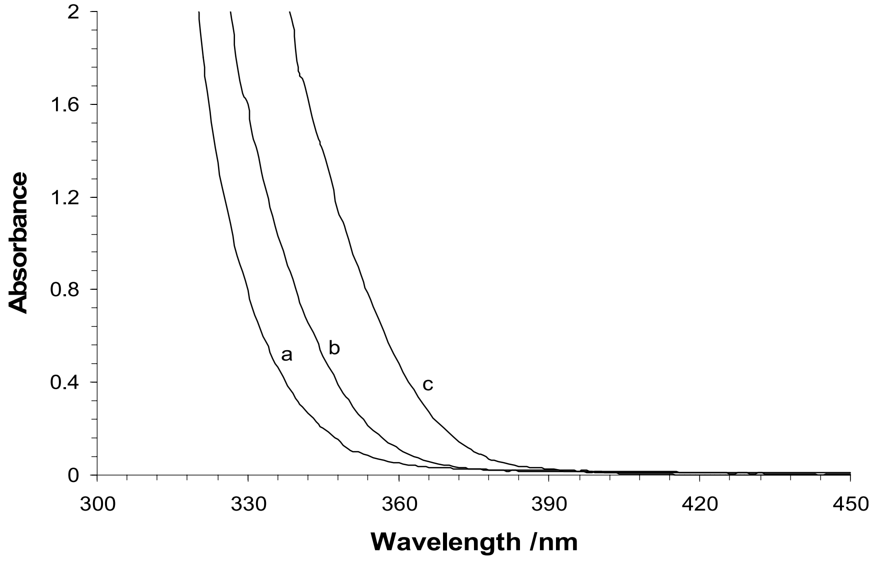

Fig. 2. UV spectra of (a) 2,4-BDE, (b) 3,5-BDE, (c) 4,4′-BDE (5.04×10^{-3} M) in trifluoroacetic acid.

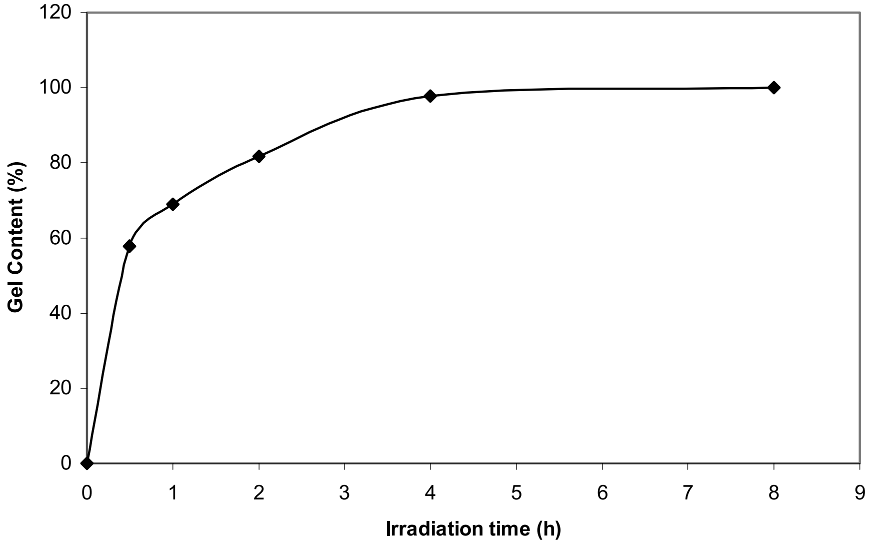

Fig. 3. Variation of gel content with irradiation time for PET/4,4′BDA-4 films irradiated with LI UV lamps.

absorption with a shift to higher wavelength and color formation (absorption above 400 nm).

3.5. Thermal analysis of photoirradiated PET copolymers

Table 2 shows the DSC results for photoirradiated PET/4,4′BDA-4 copolymer films along with those for a PET control film. The glass transition temperature (T_g) for the unirradiated PET/4,4′BDA-4 film was 76 °C, which is about the same as for the PET control film. Irradiation of the PET/4,4′BDA-4 film with LI UV lamps for 8 h increases the T_g to 81 °C, also irradiation of the PET/4,4′BDA-4 film led to considerable lowering of the heat of crystallization (ΔH_c) and heat of fusion (ΔH_m), indicating that the formation of crosslinks disrupts the crystallization of PET. There is a decrease in melting temperature (T_m) for irradiated PET/4,4′BDA-4 but no change in T_m for PET control and PET/2,4BDE-4 for irradiation for up to 8 h.

The thermal behaviors of amorphous photoirradiated PET copolymers were discussed above. Two experiments were done in order to investigate the crystallization and thermal behaviors of photoirradiated PET copolymers before and after thermal annealing: (1) Amorphous PET/4,4′BDA-4 was annealed and then irradiated; (2) amorphous PET/4,4′BDA-4 was irradiated and then annealed. Fig. 6 shows DSC scans for PET/4,4′BDA-4 annealed at 120 °C for 2 h with and without exposure to HI UV lamp at 85 °C for 15 min. The annealed PET/4,4′BDA-4 without exposure

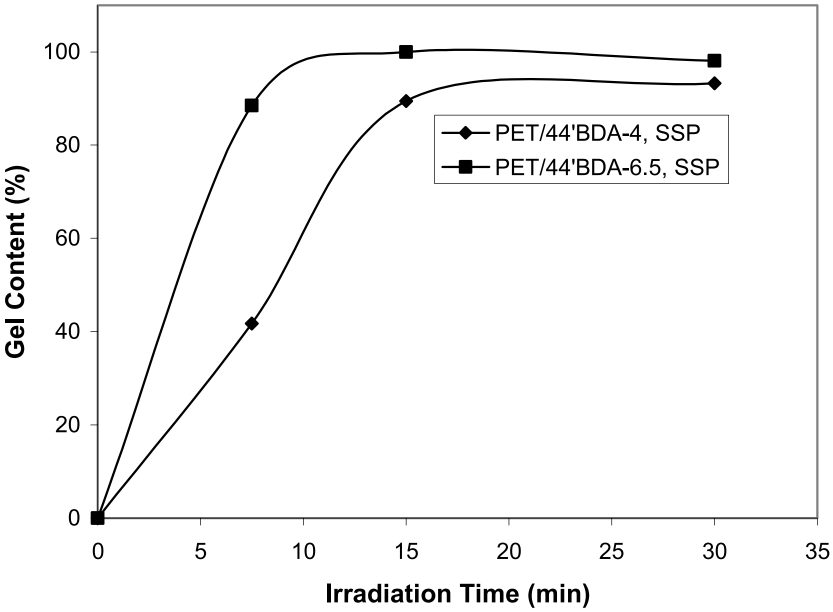

Fig. 4. Variation of gel content with irradiation time for PET 4,4′BDA-4 and PET/4,4′BDA-6.5 films irradiated with HI UV lamp.

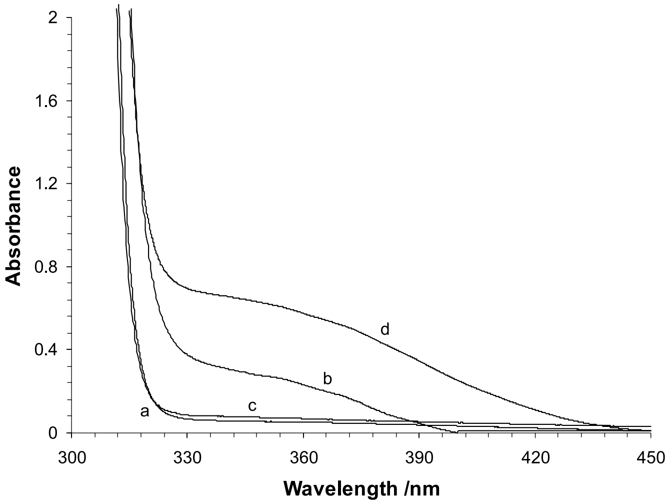

Fig. 5. UV spectra of photoirradiated and unirradiated PET/BDA copolymer films, irradiation under HI UV lamp for 15 min in air, (a) PET (b) PET/4,4′BDA-4 (c) irradiated PET (c) irradiated PET/4,4′BDA-4.

to UV shows a small crystal melting at about 129 °C, which is associated with the annealing temperature [27], and larger melting transition at about 247 °C. Annealing and then exposure to UV results in a secondary crystal melting at about 131 °C and a broad primary crystal melting at about 234 °C. This double melting behavior of glass state PET has been attributed by different authors to partial melting of crystallites formed at the annealed temperature followed by a recrystallization during scanning [27]. Most crystallites recrystallize into more thermally stable crystallites during scanning and thus melt at a higher temperature. When the PET copolymer is crosslinked, the recrystallization process during DSC scanning is inhibited (due to reduced chain mobility). Thus, less perfect crystallites are formed which lead to the broading and lowering of the melting point. Fig. 6 shows a cooling scan of PET/4,4′BDA-4 annealed at 120 °C for 2 h with and without exposure to UV light. The photoirradiated sample shows an earlier crystallization temperature than non-photoirradiated counterpart, probably indicating that crosslinks act as nuclei (impurities) to initiate faster crystallization of polymer. The other interpretation for broadening or lowering of the melting transition for photoirradiated PET copolymer is that the benzophenone triplet state ($E_T = 285 - 295$ kJ/mol [28]) transfers energy to the lower triplet excited state in the dialkylterephthalate chromophores ($E_T = 285$ kJ/mol [29]) followed by chain cleavage and concomitant formation of smaller, less well-ordered crystals with lower melting temperatures.

Table 3 shows the DSC data for amorphous PET and PET/4,4′BDA-4 polymers irradiated at room temperature for different times under HI UV lamp and then annealed at 130 °C for 2 h. Irradiated and unirradiated PET samples showed a small difference in thermal behavior. UV irradiation of PET/4,4′BDA-4 leads to crosslinking in PET segments. During annealing, crystallization becomes more difficult and leads to a decrease and broadening of the melting peak pattern compared to unirradiated PET/4,4′BDA-4. However, crystallinity based on melting enthalpies from the DSC scans for both irradiated and unirradiated samples are the same. Wide-angle X-ray diffraction spectra of both the samples show similar patterns which indicated that the crystal structure does not change significantly after photoirradiation.

TGA data show that the decomposition temperatures (T_d for 5% weight loss) were about the same for the linear PET and irradiated crosslinked polymers. However, the irradiated polymers showed earlier decomposition temperatures

Table 2
DSC Results for photoirradiated PET and PET/4,4′BDA-4 films

	Irradiation time (h), LI UV	T_g (°C)	T_c (°C)	ΔH_c (J/g)	T_m (°C)	ΔH_m (J/g)
PET	0	76.0	122.2	22.1	253.0	44.8
	8	74.8	124.4	18.6	254.0	36.4
PET/44′B DA-4	0	76.7	129.8	23.1	246.7	40.3
	0.5	77.1	133.0	18.6	240.0	32.6
	1	76.9	132.2	20.9	240.8	30.6
	2	81.0	139.6	15.4	232.8	26.6
	4	80.2	137.6	11.0	234.3	22.8
	8	80.6	146.6	5.4	228.7	17.7

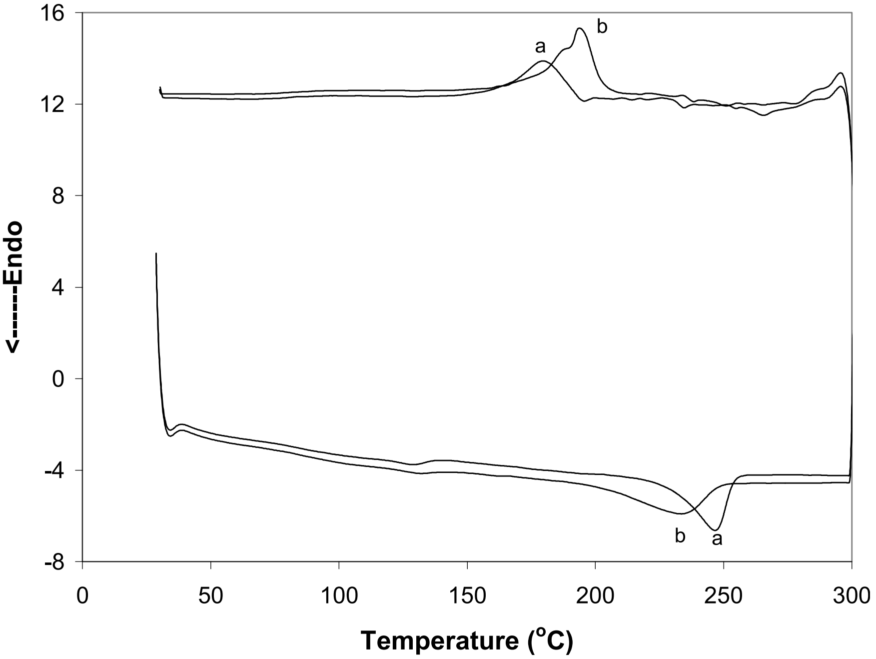

Fig. 6. DSC scans (heating and cooling) for amorphous PET/44′BDA-4 annealed at 120 for 2 h and photoirradiated at 85 °C under HI UV lamp for 15 min. Unexposed to UV lamp (a); exposed to UV lamp (b).

for 2.5% weight loss (not shown), especially for PET/4,4′BDA-18 copolymer, in which a 14 °C drop was observed relative to the unirradiated control. The polymer has the largest weight percent (18 wt%) of incorporated BDA.

3.6. Crosslinking mechanism of PET copolymer

Fig. 7 shows FTIR spectra of a PET/4,4′BDA-18 (non-SSP) amorphous film before and after UV irradiation. The decrease in absorption intensity at 1670 cm^{-1} and increase in intensity at 3460 cm^{-1} are indicative of the conversion of ketone groups to hydroxyl groups. Scheme 1 suggests a possible mechanism for photocrosslinking of those copolymers. Photoirradiation of the benzophenone chromophore in PET copolymers excites the benzophenone chromophore to an excited singlet state S_1 $\{(n, \pi^*)$ or $(\pi, \pi^*)\}$. Intersystem crossing (ISC) from S_1 to the triplet state T_1 (n, π^*) is very fast. It occurs in less than 10^{-11} s [18]. The triplet state, T_1 (n, π^*) can then go back to the ground state by one or more of several mechanisms: radiationless deactivation (intersystem crossing), self-quenching, triplet–triplet annihilation, or energy transfer quenching [18]. It can also abstract hydrogen from a hydrogen-donating segment (Scheme 5). Crosslinking can then occur by up to three radical coupling paths of the two different polymer radicals. Presumably back hydrogen atom transfer may also occur.

Table 3
DSC results for annealed (130 °C, 2 h) photoirradiated PET and PET/4,4′BDA-4 films at different irradiation times

Samples	Irradiation time (min), HI UV	T_m (°C)	ΔH (J/g)
PET	0	254.2	37.9
	30	253.5	37.5
PET/44′BDA-4	0	246.0	35.5
	15	232.6	34.5

We also UV irradiated PET/BP-5, a polymer in which PET was melt blended with benzophenone (BP, 5 wt%). No gel formation was observed upon 8 h irradiation under low intensity UV lamps, while PET/4′4′BDA-4 showed 100% gel content when irradiated under the same conditions. UV absorption spectra of a PET/BP-5 amorphous thin film before and after washing with acetone showed a considerable decrease of benzophenone UV absorption around 360 nm. Presumably benzophenone and PET polymer were phase separated and benzophenone migrated to the surface, where it could not induce crosslinking and could be removed by acetone washing. We also expect a reduction in crosslinking efficiency in these blends because benzophenone ketyl radicals in the blends have two of three possible coupling pathways, dimerization to benzpinacol and coupling to a polymer centered radical, that do not lead to crosslinked chains. Only coupling of polymer centered radicals affords crosslinks.

3.7. Dynamic mechanical analysis

Fig. 8 shows the storage modulus and tan δ values of PET and PET/4,4′BDA-4 irradiated in unconstrained states. The storage modulus of photoirradiated PET/4,4′BDA-4 is slightly higher than that of unirradiated PET/4,4′BDA-4

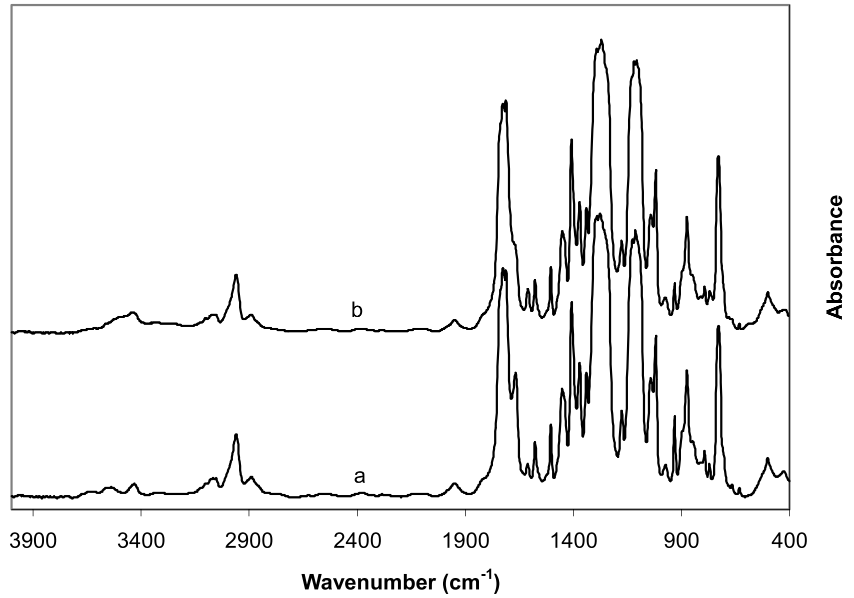

Fig. 7. FTIR spectra of PET/4,4′BDA-18 film before (a) and after photoirradiation (b) for 30 min with HI UV lamp.

and PET control below 80 °C. Between 80 and 120 °C, photoirradiated PET/4,4′BDA-4 has significantly high storage modulus than the other two. Thus, the irradiated PET/4,4′BDA-4 has better mechanical properties at high temperature. The maximum tan *δ* value of irradiated PET/4,4′BDA-4 occurs at 102 and 8 °C higher than for unirradiated PET/4,4′BDA (94 °C) and 9 °C higher than it occurs for irradiated PET (93 °C). This indicates the occurrence of crosslinking of amorphous domains of PET/4,4′BDA-4, and this crosslinking inhibits the segmental motion of chains and leads to a higher temperature of occurrence of the maximum tan *δ* value.

1. Generation of Reactive n,π* benzophenone triplet state, BP (T1) :

$$\text{BP }(S_0) \xrightarrow[> 340\text{ nm}]{h\upsilon} \text{BP }(S_1) \xrightarrow{< 10^{-11}\text{ sec}} \text{BP }(T_1)$$

2. Crosslinking by Radical Coupling:

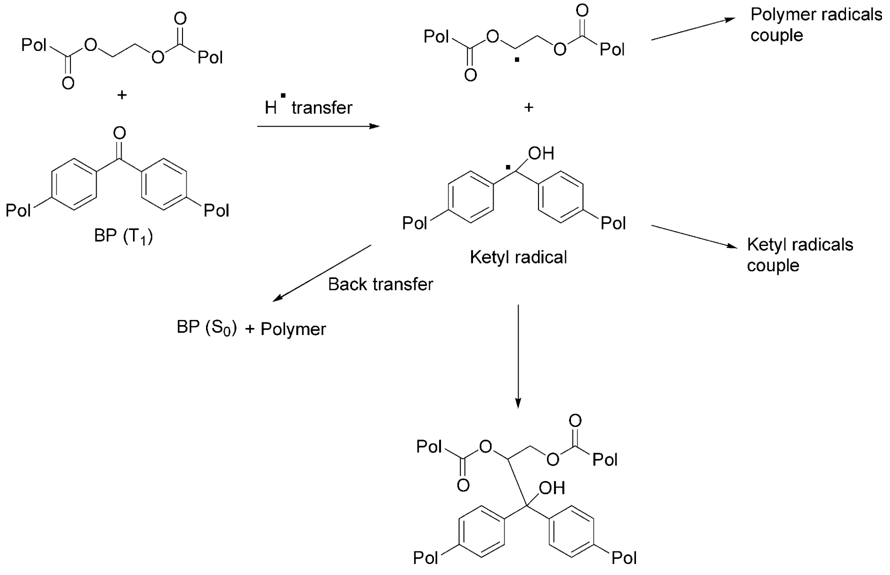

Scheme 5. Possible mechanism for crosslinking of PET copolymer with benzophenone chromophore.

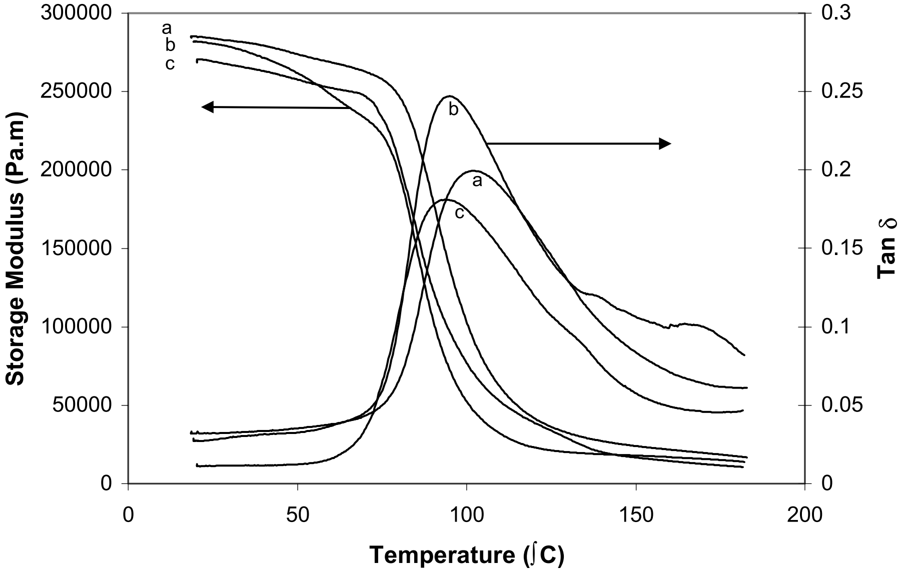

Fig. 8. DMA study of photoirradiated PET and PET/4,4′BDA-4 (200 μm) in unconstrained state. PET/BDA-4 annealed and irradiated at 185 °C for 15 min with filtered HI UV lamp (a); PET/4,4′BDA-4 annealed and irradiated at 185 °C for 15 min (b); PET annealed and irradiated at 185 °C for 15 min, with filtered HI UV lamp (c).

4. Conclusions

Benzophenone dicarboxylate derivatives were readily incorporated into the PET backbone or as pendent groups by transesterification. The presence of covalently bound benzophenone chromophores in these PET copolymers leads to a photocrosslinking reaction in the solid state, probably by a hydrogen-abstraction mechanism. The crosslinking rate depends on the concentration and the structure of the chromophore, and on the UV light source. PET with 4,4′-BDA or 4,4′-BDE incorporated shows faster photocrosslinking than PET with 2,4- and 3,5-BDE incorporated. This is probably mainly due to the stronger absorption of the 4,4′-disubstituted chromophore although more exotic explanations have not been ruled out. Blends of PET and benzophenone itself did not crosslink upon UV irradiation. Photoirradiated PET copolymers have higher storage moduli and increased glass transition temperatures compared to unirradiated copolymers. Overall, covalently incorporating benzophenone chromophores followed by UV irradiation above about 315 nm provides a simple, reliable, and inexpensive method for improving the thermal and mechanical properties of PET.

Acknowledgements

We thank David Rhoades and Prof Joshua Otaigbe for DMA measurements.

References

[1] Wu Q, Qu B. J Appl Polym Sci 2002;85:1581–6.
[2] Qu B, Xu Y, Ding L, Ranby B. J Polym Sci, Part A: Polym Chem 2000;38:999–1005.
[3] Wu Q, Qu B. Polym Eng Sci 2001;41(7):1220–6.
[4] Wu Q, Qu B, Xu Y, Wu Q. Polym Degrad Stab 2000;68:97–102.
[5] Yamaoka H, Ikeda T, Okamura S. Macromolecules 1977;10:717.
[6] Scaiano JC, Netto-Ferreira JC, Becknell AF, Small RD. Polym Eng Sci 1989;29(14):942–4.
[7] Jin Q, Yamashita T, Horie K. J Polym Sci, Part A: Polym Chem 1994;32:503–11.
[8] Minto F, Gleria M, Bertani R, Noto VD, Vidali MJ. Inorg Organomet Polym 1998;8(2):67–88.
[9] Wycisk R, Pintauro PN, Wang W, O'Connor S. J Appl Polym Sci 1996;59:1607–17.
[10] Takatani K, Kawatsuki N, Yamamoto T. Macromol Chem Phys 1998;199:1759–63.
[11] Kawatsuki N, Takatani K, Yamamoto T, Sangen O. Macromol Chem Phys 1997;198:2853–66.
[12] Vargas M, Collard DM, Liotta CL, Schiraldi DA. J Polym Sci, Part A: Polym Chem 2000;38:2167–76.
[13] Jones JR, Liotta CL, Collard DM, Schiraldi DA. Macromolecules 1999;32:5786–92.
[14] Jones JR, Liotta CL, Collard DM, Schiraldi DA. Macromolecules 2000;33:1640–5.
[15] Chang JH, Kim SJ, Joo YL, Im S. Polymer 2004;45:919–26.
[16] Schiraldi DA, Zeng J, Kumar S. POSS Nanotechnol Conf 2002.
[17] Bikiaris DN, Karayannidis GP. Polym Int 2003;52(7):1230–9.
[18] Rabek JF. Mechanisms of photophysical process and photochemical reactions in polymer. New York: Wiley; 1987.
[19] Du Pont de Nemours, E.I., and Co. NL 6606547; 1966.
[20] Uno K. Nippon Setchaku Gakkaishi 1990;26(1):4–13.
[21] Uno K. Nippon Setchaku Gakkaishi 1990;26(2):51–7.
[22] Cheung PR, Roberts CW. J Appl Polym Sci 1979;24:1809–30.
[23] Moshchinskaya NK, Silin NF, Dmitrenko EE, Liberzon VA, Lokshin GB, Korchagina AM. Neftekhimiya 1962;2:54109.

[24] Lozano AE, Abajo J, Campa JG. J Polym Sci, Part A: Polym Chem 1993;31:1203–10.

[25] (a) Kotek R, Pang K, Schmidt B, Tonelli A. J Polym Sci, Part B: Polym Phys 2004;42(23):4247–54.
(b) Aharoni SM. Makromol Chem 1978;179:1867–71.

[26] (a) Dellinger JA, Roberts CW. J Appl Polym Sci 1981;26:321–42.
(b) Merrill RG, Roberts CW. J Appl Polym Sci 1977;21:2745–68.

[27] (a) Groeninckx G, Reynaers H, Berghmans H, Smets G. J Polym Sci Part B: Polym Phys 1980;18(6):1311–24.
(b) Groeninckx G, Reynaers H. J Polym Sci, Part B: Polym Phys 1980;18(6):1325–41.
(c) Reberts RC. Polymer 1969;10:117.
(d) Holdsworth PJ, Turner-Jones A. Polymer 1971;12:195.
(e) Bell JP, Murayama T. J Polym Sci A-2 1969;7:1059.
(f) Reberts RC, Reberts RC. J Polym Sci, Part B: Polym Phys 1970;8: 381.
(g) Sweet GE, Bell JP. J Polym Sci A-2 1972;10:1273.
(h) Nealy DL, Davis TG, Kibler CJ. J Polym Sci A-2 1970;8:2141.

[28] Liska R. J Polym Sci, Part A: Polym Chem 2004;42(9): 2285–301.

[29] Takai Y, Mizutani T, Ieda M. Jpn J Appl Phys 1978;17(4): 651–8.